Chapter 1
Historical Overview and General Methods of Membrane Potential Imaging

Oliver Braubach, Lawrence B. Cohen, and Yunsook Choi

Abstract Voltage imaging was first conceived in the late 1960s and efforts to find better organic voltage sensitive dyes began in the 1970s and continue until today. At the beginning it was difficult to measure an action potential signal from a squid giant axon in a single trial. Now it is possible to measure the action potential in an individual spine. Other chapters will discuss advances in voltage imaging technology and applications in a variety of biological preparations. The development of genetically encoded voltage sensors has started. A genetically encoded sensor could provide cell type specific expression and voltage recording (see Chap. 20).

Optimizing the signal-to-noise ratio of an optical recording requires attention to several aspects of the recording apparatus. These include the light source, the optics and the recording device. All three have improved substantially in recent years. Arc lamp, LED, and laser sources are now stable, more powerful, and less expensive. Cameras for recording activity have frames rates above 1 kHz and quantum efficiencies near 1.0 although they remain expensive. The sources of noise in optical recordings are well understood. Both the apparatus and the noise sources are discussed in this chapter.

Keywords History • Richard Keynes • David Hill • Ichiji Tasaki • Dora Rosental • David Gilbert • Shot noise • Signal-to-noise ratio • Out-of-focus blurring • Scattering

O. Braubach • Y. Choi
Center for Functional Connectomics, Korea Institute of Science and Technology (KIST), Seoul 136-791, Korea

L.B. Cohen (✉)
Center for Functional Connectomics, Korea Institute of Science and Technology (KIST), Seoul 136-791, Korea

Department of Cellular and Molecular Physiology, Yale University School of Medicine, New Haven, CT 06520, USA
e-mail: lawrence.b.cohen@hotmail.com

M. Canepari et al. (eds.), *Membrane Potential Imaging in the Nervous System and Heart*, Advances in Experimental Medicine and Biology 859,
DOI 10.1007/978-3-319-17641-3_1

1 Motivation

Several factors make optical methods interesting to physiologists and neuroscientists. First, is the possibility of making simultaneous measurements from multiple sites. Because many different neurons in a nervous system are active during each behavior, it is obviously important to be able to monitor activity from many cells simultaneously. Similarly, different parts of a neuron may perform different functions and again it would be essential to make simultaneous observations over the whole structure of the neuron. Finally, many different brain regions are simultaneously active during behaviors and recording of population signals from these regions would be useful.

Second, optical measurement can be made with very high time resolution. Some voltage sensitive dyes are known to respond to changes in membrane potential extremely rapidly, with time constants of less than 1 μs. Other indicators of activity, such as hemodynamic changes, monitored as intrinsic signals, can be much slower, with latencies and durations in the range of seconds, but even so these recordings reflect real-time measurements of events in the brain. Third, optical measurements are in some sense non-invasive; recordings can be made from cells and processes too small for electrode measurements; these include T-tubules, presynaptic terminals, and dendritic spines. On the other hand, optical measurements using extrinsic dyes and proteins can be invasive if they cause pharmacological or photodynamic effects. The degree of this kind of invasiveness varies from relatively innocuous, to measurements where pharmacology and photodynamic damage are important factors, a subject discussed in detail in later chapters.

The above three factors are clearly attractive because the use of voltage imaging has grown dramatically since its beginnings in the 1970s. Nonetheless it is important to note that optical methods cannot be used to record from deep in a tissue, an important capability which other, slower, imaging methods such as fMRI and 2-deoxyglucose do provide.

Three kinds of optical signals have been extensively used to monitor activity; indicators of membrane potential, intracellular ion concentrations, and intrinsic signals. This book chapter is an historical and technical introduction of voltage imaging.

2 History

2.1 Early Milestones in Imaging Activity

The first optical signals detected during nerve activity were light scattering changes that accompany trains of stimuli to nerves (Hill and Keynes 1949; Hill 1950). During and following the stimuli there is first an increase in scattering followed by a slower decrease lasting many tens of seconds (Fig. 1.1a). On the top left is a

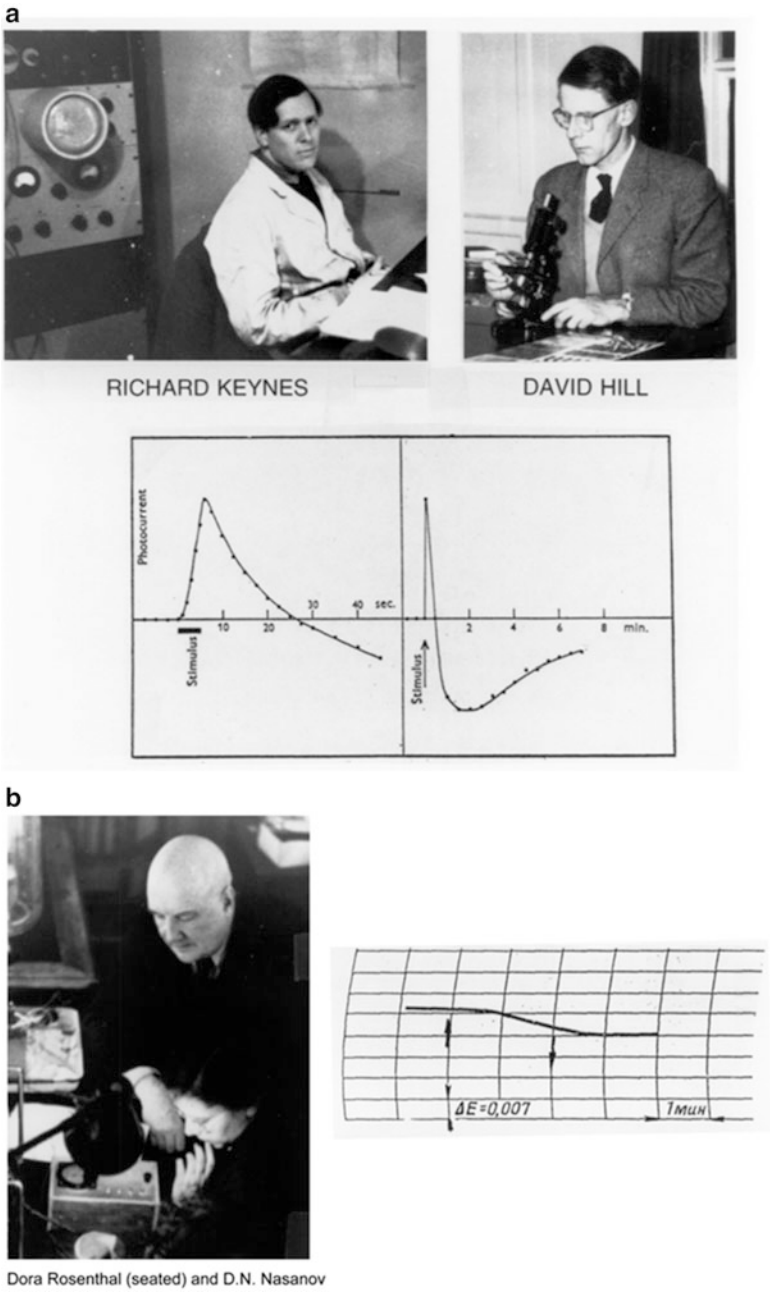

Fig. 1.1 (**a**) *Top*. Photographs of Richard Keynes and David Hill. *Bottom panel*. A *Carcinus maenas* leg nerve was stimulated 250 times during the bar labeled stimulus. The stimulus resulted in an increase in scattering that lasted about 20 s. This was followed by a scattering decrease which persisted for several minutes. From Hill and Keynes (1949). (**b**) A photograph of D.N. Nasonov and Dora Rosenthal taken in 1956 together with a recording of the change in Direct Turquoise absorption as a result of stimulating a crab axon 50 times per second for 2 min (6,000 stimuli). The optical recording is from Levin et al. (1968)

photograph of Richard Keynes (together with an oscilloscope) taken at the time of those measurements; on the top right is a photograph of David Hill taken about 20 years later. In the bottom panel is the recording of light scattering from a whole crab leg nerve as a function of time during and following a train of 250 stimuli. The light scattering response is shown on two time bases.

Starting at about the same time and continuing into the 1960s, scientists at the Institute of Cytology in Leningrad began measuring changes in the optical properties of dye stained nerves (Nasonov and Suzdal'skaia 1957; Vereninov et al. 1962; Levin et al. 1968). Again they used relatively long stimulus trains and recorded signals with time courses of tens of seconds. The photograph in Fig. 1.1b includes two of the scientists: D. N. Nasonov (standing) and Dora Rosenthal (seated). On the right is a recording from Levin et al. (1968) illustrating the change in absorption of the dye Direct Turquoise from an isolated crab axon.

With the introduction of signal averaging to biological research it became possible to measure signals that were much smaller. One could then look for signals that occurred coincident with the action potential. This led to the discovery of changes in light scattering and birefringence that accompany the action potentials in nerves and single axons (Cohen et al. 1968). Figure 1.2a shows the first measurement of the birefringence signal from a squid giant axon made at the Laboratory of the Marine Biological Association in 1967. The signal was very small; the fractional change, $\Delta I/I$, was only 1 part in 100,000. And, 20,000 trials had to be averaged to achieve the signal-to-noise ratio shown in the figure. Brushing aside the tiny size of the signals, David Gilbert (Fig. 1.2b; personal communication) pointed out that optical signals might be used to follow activity in the nervous system. Soon thereafter Ichiji Tasaki (Fig. 1.2b) and collaborators (Tasaki et al. 1968) discovered fast changes in the fluorescence of axons that were stained with dyes. Several years later changes in dye absorption (Ross et al. 1974) and birefringence (Ross et al. 1977) were also found. Almost all of these dye signals were shown to depend on changes in membrane potential (Davila et al. 1974; Cohen et al. 1974; Salzberg and Bezanilla 1983) a conclusion that is now widely accepted. However, there was early disagreement (Conti et al. 1971) and Ichiji was always unconvinced.

In 1971 we began a deliberate search for larger optical signals by screening many dyes. After a few years of testing and ~1,000 dyes we had obtained signals that were about 100 times larger than the intrinsic signals described above. One hundred times larger doesn't mean that the signals are now large. Care is still needed to optimize the measurement signal-to-noise ratio. The second section of this chapter together with other chapters provide information about the needed optimization. Because of this improvement in signal size, we were able to record optical signals from a smaller membrane area and with higher time resolution. The top panel of Fig. 1.3 illustrates a single trial absorption signal from a single action potential in a 50 μm diameter barnacle neuron made with the merocyanine dye whose structure is illustrated. The five adults on the right hand side of the photograph at the bottom were in large part responsible for the dye screening. Other important contributors during those early years (not shown) were Vicencio Davila, Jeff Wang, Ravinder Gupta and Alan Waggoner.

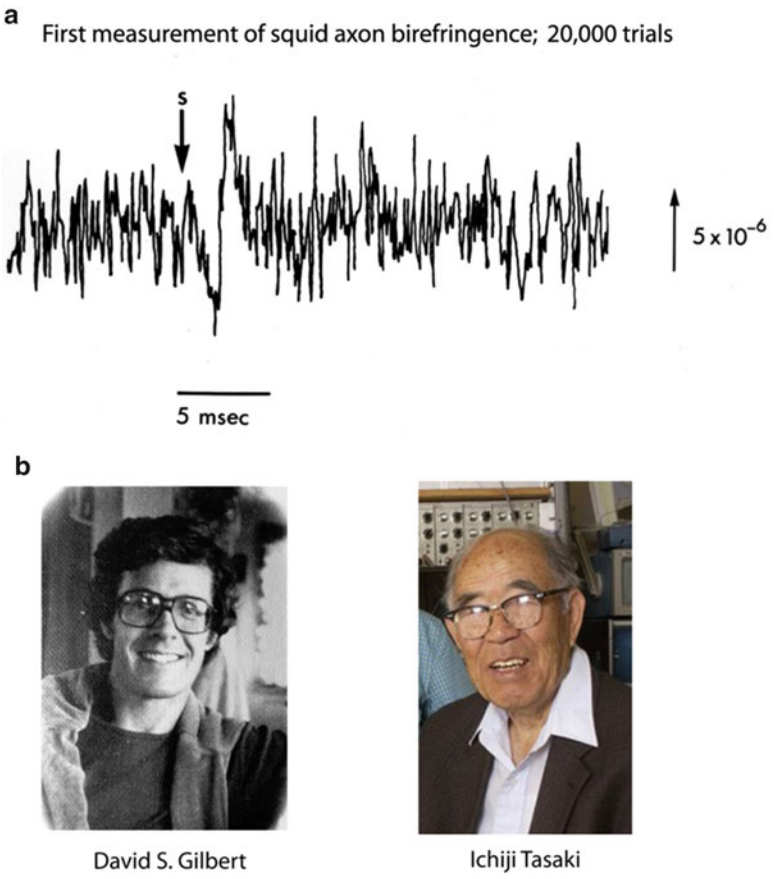

Fig. 1.2 (**a**) The first recording of an optical signal (birefringence) from an individual axon on a time scale appropriate for measuring the time course of the signal during the action potential. 20,000 trials were averaged. In this and subsequent figures the size of the *vertical line* represents the stated value of the fractional change in intensity (ΔI/I or ΔF/F). (L.B. Cohen and R.D. Keynes, unpublished result). (**b**) Photographs of David Gilbert and Ichiji Tasaki

2.2 *Ion Sensitive Dyes and Their Comparison with Voltage Sensitive Dyes*

The first attempt to use organic optical indicators of intracellular ion concentration were measurements of calcium with the dye murexide (Jobsis and O'Connor 1966). Ironically, those results are now thought to be an artifact (Maylie et al. 1987). Ashley and Ridgway (1970) later introduced the use of the photoprotein aequorin. Following the suggestion of John Cooper (personal communication), the Arsenazo class of calcium dyes was introduced (Brown et al. 1975). More recently, Roger Tsien and collaborators have developed a large number of widely used ion indicator dyes based on the chemical structure of the chelator EGTA (e.g. Tsien 1989).

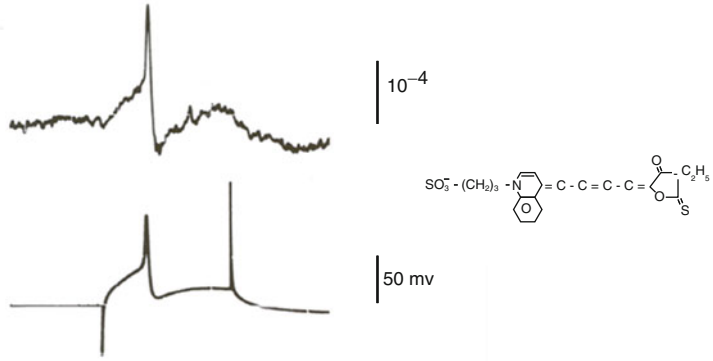

Absorption signals from a single neuron in a barnacle ganglion.

Fig. 1.3 On the *top* is an absorption change measured during a single action potential from a cell body in a barnacle supraesophageal ganglion. The structure of the absorption dye, synthesized by Jeff Wang and Alan Waggoner, is illustrated at the *top*. In the photograph are, from the *left*, Naoko Kamino, Kyoko Kamino, Irit Grinvald, Eran Grinvald, Amiram Grinvald, Larry Cohen, Kohtaro Kamino, Kaeko Kamino, Brian Salzberg and Bill Ross. The photograph, made by Sarah Lesher, is from 1976. The optical recording is from Salzberg et al. (1977)

Figure 1.4 illustrates two time course comparisons between voltage, calcium, and intrinsic signals. The top pair compares voltage and calcium signals from the same location on a turtle olfactory bulb. The signals are in response to a shock to the olfactory nerve. The voltage sensitive dye signal rises faster and falls faster than the calcium signal. Some of the slowness of the calcium signal is thought to result

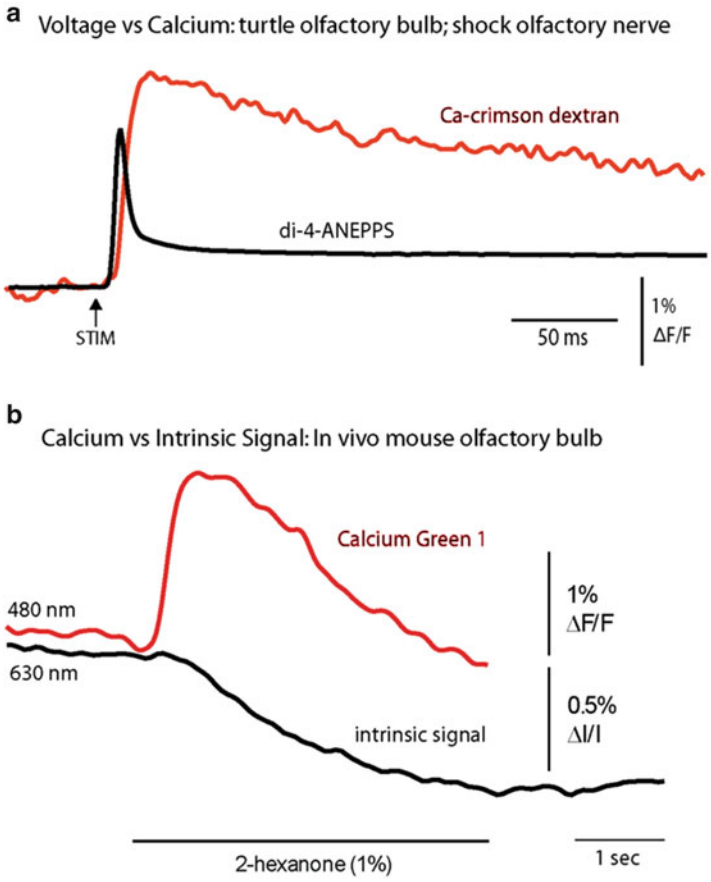

Fig. 1.4 Comparisons of voltage, calcium, and intrinsic imaging signals. (**a**) A comparison of the time course of a voltage and a calcium dye signal from the same location near the merger of the olfactory nerve and the olfactory bulb in an *in vitro* turtle preparation. The voltage signal is faster (M. Wachowiak and L. B. Cohen, unpublished). (**b**) A comparison of the time course of the calcium signal and the intrinsic imaging signal in a mouse olfactory bulb glomerulus in response to the odorant, 2-hexanone. The intrinsic imaging signal is substantially slower than the calcium signal. (Modified from Wachowiak and Cohen 2003)

from the dye response itself and some from the time taken by the cells to bring their calcium concentration back to its original level. The bottom pair of traces compares a calcium signal and an intrinsic signal (Blasdel and Salama 1986; Grinvald et al. 1986) from the same glomerulus in a mouse olfactory bulb. Here the stimulus was an odorant presented to the nose. The calcium signal reaches a peak in less than 0.5 s while the intrinsic signal doesn't reach its peak until about 5 s after the stimulus onset.

2.3 *Multi-site Measurements of Brain Activity*

The first multi-site measurements of brain activity were made by Schuette et al. (1974) who used an image intensifier and camera tube to monitor changes in NADH fluorescence from cortex during epileptic seizures. This was followed by methods using several individual silicon photodiodes (Salzberg et al. 1977), and later by a variety of photodiode arrays, camera tubes, CCD and CMOS cameras.

3 Measurement Principles

Even though the changes in membrane potential during action potentials and synaptic activity are small in mV, they are giant in volts/cm because the membrane is very thin. Thus, 100 mV across 3 nm is 300,000 V/cm, a voltage gradient long known to be able to alter the spectral properties of merocyanine dyes (Labhart 1963; Bucher et al. 1969). This direct effect of voltage on dye spectra, called electrochromism, is one mechanism thought to give rise to signals from organic voltage sensitive dyes (Loew et al. 1985). Other mechanisms with spectral supporting evidence are voltage sensitive shifts in monomer-dimer equilibria (Waggoner and Grinvald 1977) and dye rotation in the electric field (Conti 1975; Fromherz et al. 1991). Because the electric field change is so large, it is perhaps not surprising that we were able to measure signals in ~500 of the ~2,000 dyes that were tested on squid giant axons.

Action potential propagation and synaptic currents also give rise to extracellular and intracellular currents which means that there will also be voltage gradients in these locations. However these extracellular currents flow over distances of mm (rather than nm) and thus the voltage gradients are smaller by six orders of magnitude. It is for this reason that the voltage sensitive dye signals are presumed to arise solely from changes in dye molecules embedded in or directly adjacent to the membrane.

4 The Definition of a Voltage Sensitive Dye

The voltage-sensitive dye signals described in this book are “fast” signals (Cohen and Salzberg 1978) that are presumed to arise from membrane-bound dye. Figure 1.5, top, illustrates the kind of result that is used to define a voltage sensitive dye. In a giant axon from a squid, these optical signals are fast, following membrane potential with a time constant of <10 μs (Loew et al. 1985). The dye signals have a time course that is qualitatively different from the time course of the ionic currents or the membrane permeability changes. With almost all of the tested dyes the signal size is linearly related to the size of the change in potential (e.g. Gupta et al. 1981).

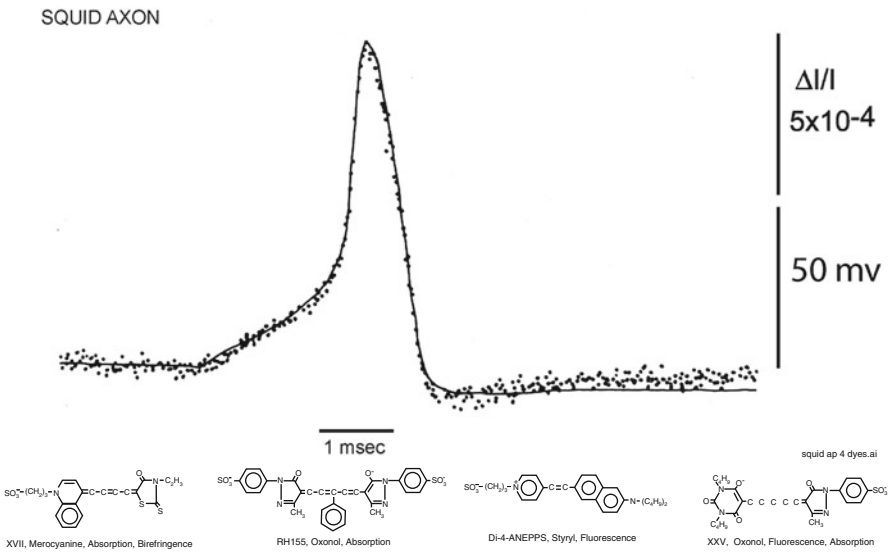

Fig. 1.5 *Top*. Changes in absorption (*dots*) of a giant axon stained with a merocyanine dye, XVII, (*bottom left* dye) during a membrane action potential (*smooth trace*) recorded simultaneously. The change in absorption and the action potential had the same time course. The response time constant of the light measuring system was 35 μs; 32 sweeps were averaged. *Bottom*. Examples of four different chromophores that have been used to monitor membrane potential. The merocyanine dye, XVII (WW375), and the oxonol dye, RH155, were commercially available as NK2495 and NK3041 from Nippon Kankoh-Shikiso Kenkyusho Co. Ltd., Okayama, Japan. The oxonol, XXV (WW781) and styryl, di-4-ANEPPS, are available commercially as dye R-1114 and D-1199 from Invitrogen (Molecular Probes), Junction City, OR

Thus, these dyes provide a direct, fast, and linear measure of the change in membrane potential of the stained membranes.

A direct comparison of membrane potential and voltage-sensitive dye signal like that illustrated in Fig. 1.5 cannot often be made. Several of the following chapters discuss the important issues involved in interpreting less direct comparisons.

Several organic voltage-sensitive dyes have been used to monitor changes in membrane potential in a variety of preparations. Figure 1.5, bottom, illustrates four different chromophores (the merocyanine dye, XVII, was used for the measurement illustrated in Fig. 1.5, top). The merocyanine dye, XVII (WW375), and the oxonol dye, RH155 were commercially available as NK2495 and NK3041 from Nippon Kankoh-Shikiso Kenkyusho Co. Ltd., Okayama, Japan. The oxonol, XXV (WW781) and styryl, di-4-ANEPPS, are commercially available as dye R-1114 and D-1199 from Invitrogen (Molecular Probes), Junction City, OR. For each of the four chromophores approximately 100 analogues have been synthesized in an attempt to optimize the signal-to-noise ratio. (This screening was made possible by synthetic efforts of three laboratories: Jeff Wang, Ravender Gupta and Alan Waggoner then at Amherst College; Rina Hildesheim and Amiram Grinvald at the Weizmann Institute; and Joe Wuskell and Leslie Loew at the University of

Connecticut Health Center.) For each of the chromophores, there were 10 or 20 dyes that gave approximately the same signal size on squid axons (Gupta et al. 1981). However, dyes that had nearly identical signal size on squid axons often had very different responses on other preparations, and thus tens of dyes usually have to be tested to obtain the largest possible signal. A common failure was that the dye did not penetrate through connective tissue or along intercellular spaces to the membrane of interest.

The following rules-of-thumb seem to be useful. First, each of the chromophores is available with a fixed charge, which is either a quaternary nitrogen (positive) or a sulfonate (negative). Generally the positive dyes have given larger signals when dye is applied either extracellularly or intracellularly in vertebrate preparations. Second, each chromophore is available with carbon chains of several lengths. The more hydrophilic dyes (methyl or ethyl) work best if the dye has to penetrate through a compact tissue (vertebrate brain) or be transported to distant branches of a dendritic tree. More hydrophobic dyes (hexyl or octyl) work best in tissue culture; in tissue culture the less hydrophobic dyes unbind rapidly.

5 Preliminary Considerations

The optical signals are small in many of the examples of voltage sensitive dye measurements given in the chapters in this book. Some examples involve fractional intensity changes, $\Delta I/I$, that are as low as 10^{-4}. In order to measure these signals, the noise in the measurements had to be an even smaller fraction of the resting intensity. In the sections that follow, some of the considerations necessary to achieve such a low noise are outlined.

5.1 Signal Type

Sometimes it is possible to decide in advance which kind of optical signal will give the best signal-to-noise ratio but, in other situations, an experimental comparison is necessary. The choice of signal type often depends on the optical characteristics of the preparation. Extrinsic birefringence signals are relatively large in preparations that, like axons, have a cylindrical shape and radial optic axis (Ross et al. 1977). However, in preparations with spherical symmetry (e.g., cell soma), the birefringence signals in adjacent quadrants will cancel (Boyle and Cohen 1980).

Thick preparations (e.g. mammalian cortex) also dictate the choice of signal. In this circumstance transmitted light measurements are not easy (a subcortical implantation of a light guide would be necessary), and the small size of the absorption signals that are detected in reflected light (Ross et al. 1977; Orbach and Cohen 1983) meant that fluorescence would be optimal (Orbach et al. 1985). Another factor that affects the choice of absorption or fluorescence is that the

signal-to-noise ratio in fluorescence is more strongly degraded by dye bound to extraneous material.

Fluorescence signals have most often been used in monitoring activity from tissue-cultured neurons. Both kinds of signals have been used in measurements from ganglia and brain slices. Fluorescence has always been used in measurements from intact vertebrate brains.

5.2 Amplitude of the Voltage Change

Activity signals are often presented as a fractional intensity change, ΔI/I. The signals give information about the time course of the potential change but no direct information about the absolute magnitude. However, in some instances, approximate estimations can be obtained. For example, the size of the optical signal in response to a sensory stimulus can be compared to the size of the signal in response to an epileptic event (Orbach et al. 1985). Or in single neuron experiments long lasting hyperpolarizing steps can be induced in the soma after blocking ionic currents and this signal can be used for calibration. Another approach is the use of ratiometric measurements at two independent wavelengths (Gross et al. 1994). However, one must know the fraction of the fluorescence that results from dye bound to active membranes *versus* dye bound to non-active membranes. This requirement is almost never met.

6 Noise

6.1 Shot Noise

The limit of accuracy with which light can be measured is set by the shot noise arising from the statistical nature of photon emission and detection. Fluctuations in the number of photons emitted per unit time occur, and if an ideal light source (e.g. a tungsten filament) emits an average of 10^{16} photons/ms, the root-mean-square (RMS) deviation in the number emitted is the square root of this number or 10^{8} photons/ms. Because of shot noise, the signal-to-noise ratio is directly proportional to the square root of the number of measured photons and inversely proportional to the square root of the bandwidth of the photodetection system (Braddick 1960; Malmstadt et al. 1974). The basis for the square root dependence on intensity is illustrated in Fig. 1.6. In the top plot, the result of using a random number table to distribute 20 photons into 20 time windows is shown. In the bottom plot the same procedure was used to distribute 200 photons into the same 20 bins. Relative to the average light level there is more noise in the top trace (20 photons) than in the bottom trace (200 photons). The improvement from A to B is similar to that

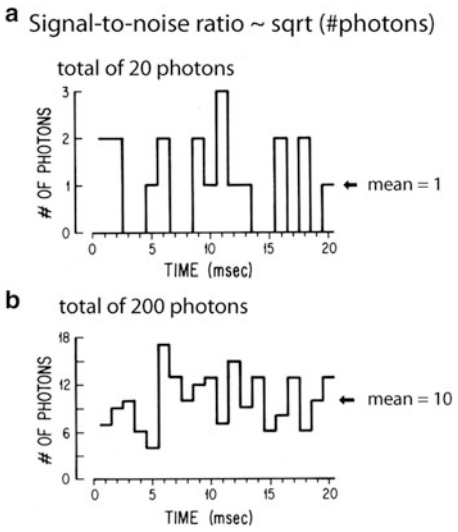

Fig. 1.6 Plots of the results of using a table of random numbers to distribute 20 photons (*top*, **a**) or 200 photons (*bottom*, **b**) into 20 time bins. The result illustrates the fact that when more photons are measured the signal-to-noise ratio is improved. The improvement is close to that expected from the known square root relationship between the signal-to-noise ratio and the measured intensity. Redrawn from Wu and Cohen (1993)

expected from the square-root relationship. This square-root relationship is indicated by the straight red line in Fig. 1.7 which plots the light intensity divided by the noise in the measurement versus the light intensity. In a shot-noise limited measurement, improvement in the signal-to-noise ratio can only be obtained by (1) increasing the illumination intensity, (2) improving the light-gathering efficiency of the measuring system, or (3) reducing the bandwidth.

6.2 The Optimum Signal to Noise Ratio

Because only a small fraction of the 10^{16} photons/ms emitted by a tungsten filament source will be measured, a signal to noise ratio of 10^8 (see above) cannot be achieved. A partial listing of the light losses follows. A 0.9 NA lamp collector lens would collect 10 % of the light emitted by a point source. Only 20 % of that light is in the visible wavelength range; the remainder is infrared (heat). Limiting the incident wavelengths to those which elicit a signal means that only 10 % of the visible light is used. Thus, the light reaching the preparation might typically be reduced to 10^{13} photons/ms. If the light-collecting system that forms the image has high efficiency e.g., in an absorption measurement, about 10^{13} photons/ms will reach the image plane. (In a fluorescence measurement there will be much less light measured because (1) only a fraction of the incident photons are absorbed by the fluorophores, (2) only a fraction of the absorbed photons reappear as emitted photons, and (3) only a fraction of the emitted photons are collected by the objective.) If the camera has a quantum efficiency of 1.0, then, in

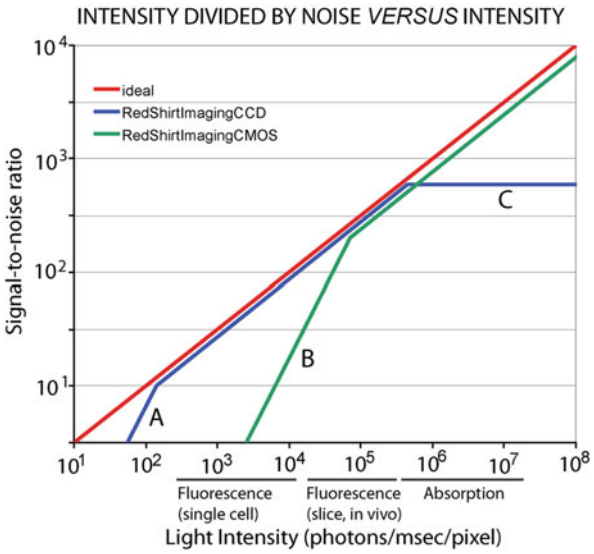

Fig. 1.7 The ratio of light intensity divided by the noise in the measurement as a function of light intensity in photons/ms/pixel. The theoretical optimum signal-to-noise ratio (*red line*) is the shot-noise limit. Two camera systems are shown, a cooled, back-illuminated, 2 kHz frame rate, 80×80 pixel CCD camera (*blue lines*) and a CMOS camera (*green lines*). The CMOS camera provides an optimal signal-to-noise ratio at higher intensities while the CCD camera is better at lower intensities. The approximate light intensity per detector in fluorescence measurements from a single neuron, fluorescence measurements from bath application of dye to a slice or *in vivo* preparation, and in absorption measurements from a ganglion or a slice is indicated along the x axis. The signal-to-noise ratio for the CMOS camera falls away at low intensities because of dark noise (*B*). The lower dark noise of the cooled CCD allows it to function at the shot-noise limit at lower intensities until read noise dominates (*A*). The CCD camera saturates at intensities above 5×10^6 photons/ms/0.2 % of the object plane (*C*)

absorption, a total of 10^{13} photoelectrons/ms will be measured. With a camera of 10,000 pixels, there will be 10^9 photoelectrons/ms/pixel. The r.m.s. shot noise will be $10^{4.5}$ photoelectrons/ms/pixel; thus the very best that can be expected is a noise that is $10^{-4.5}$ of the resting light (a signal-to-noise ratio of 90 dB). The extra light losses in a fluorescence measurement will further reduce the maximum obtainable signal-to-noise ratio.

One way to compare the performance of different camera systems and to understand their deviations from optimal (shot-noise limited) is to determine the light intensity divided by the noise in the measurement and plot that versus the number of photons reaching the each pixel of the camera. The straight red line in Fig. 1.7 is the plot for an ideal camera. At high light intensities this ratio is large and thus small changes in intensity can be detected. For example, at 10^8 photons/ms a fractional intensity change of 0.1 % can be measured with a signal-to-noise ratio of 10. On the other hand, at low intensities the ratio of intensity divided by noise is

small and only large signals can be detected. For example, at 10^4 photons/ms the same fractional change of 0.1 % can be measured with a signal-to-noise ratio of only 1 and that only after averaging 100 trials.

In addition, Fig. 1.7 compares the performance of two particular cameras, a cooled 80×80 pixel CCD camera (blue line), and a 128×128 pixel CMOS camera (green line). The CMOS camera approaches the shot-noise limitation over the range of intensities from 5×10^4 to 10^8 photons/ms/pixel. This is the range of intensities obtained in absorption measurements and fluorescence measurements on bulk-stained *in vitro* slices and intact brains. On the other hand, the cooled CCD camera approaches the shot noise limit over the range of intensities from 2×10^2 to 5×10^5 photons/ms/pixel. This is the range of intensities obtained from fluorescence experiments on processes of individual cells and neuron cell bodies.

In the discussion that follows we will indicate the aspects of the measurements and the characteristics of the two camera systems which cause them to deviate from the shot noise ideal. The two camera systems we have chosen to illustrate in Fig. 1.7 have relatively good dark noise and saturation characteristics; other cameras would be dark noise limited at higher light intensities and would saturate at lower intensities. At present there is no single camera which can cover the entire intensity range of interest to physiologists with close to shot noise limited performance.

6.3 *Extraneous Noise*

A second type of noise, termed extraneous or technical noise, is more apparent at high light intensities where the sensitivity of the measurement is high because the fractional shot noise and dark noise are low. One type of extraneous noise is caused by fluctuations in the output of the light source (see below). Two other sources of extraneous noise are vibrations and movement of the preparation. A number of precautions for reducing vibrational noise have been described (Salzberg et al. 1977, London et al. 1987). The pneumatic isolation mounts on many vibration isolation tables are more efficient in reducing vertical vibrations than in reducing horizontal movements. An improvement is air-filled soft rubber tubes (Newport Corp, Irvine, CA). For more severe vibration problems, Minus K Technology (Inglewood, CA) sells vibration isolation tables with very low resonant frequencies. For even tougher situations the Halcyonics Micro 60 (Menlo Park, CA) is an active (piezoelectric drivers) isolator and can defeat airborne vibrations as well as those transmitted from the floor (Brian Salzberg, personal communication). The increasing improvement comes at increasing cost. Nevertheless it has been difficult to reduce vibrational noise to less than 3×10^{-5} of the total light. With this amount of vibrational noise, increases in measured intensity beyond 10^9 photons/ms would not improve the signal-to-noise ratio.

6.4 Dark Noise/Read Noise

At 1 kHz frame rates the read noise is likely to be larger than the dark noise in CCD and CMOS cameras. The read noise will degrade the signal-to-noise ratio at very low light levels (<100 photons/pixel/frame for the RedShirtImaging CCD camera). The read noise of cooled CCD cameras can be substantially lower than that of large pixel CMOS cameras (Table 1.2). The larger read noise in the CMOS camera accounts for the fact that segment B in Fig. 1.7 is substantially to the right of segment A.

6.5 Preparation Movement

Preparation movement is often the limiting noise factor in wide-field *in vivo* measurements. The movement artifacts *in vivo* usually consist of irregular movements of the entire animal (less of a problem in anesthetized preparations) as well as of heart beat- and breathing-related movements of the brain. The heart beat pulsations are larger in regions with a high density of blood vessels. The heart beat- and breathing-related artifacts significantly increase their amplitudes when the skull and the *dura matter* are removed. The stability of recordings also depends on the diameter of the craniotomy. Thus, openings larger than 1 mm in diameter are often accompanied by larger movement artifacts. This noise can be reduced by covering the skull opening with 2 % agarose and a glass coverslip (Svoboda et al. 1997), by keeping the temperature of the brain surface stable (with a precision of 0.1 °C (Garaschuk et al. 2006)), and by subtraction techniques (Orbach et al. 1985).

7 Light Sources

Three kinds of sources have been used. Tungsten filament lamps are a stable source, but their intensity is relatively low, particularly at wavelengths less than 480 nm. Arc lamps are somewhat less stable but can provide higher intensity. Laser illumination can provide even more intense illumination. Newly available LED sources are bright, stable, and convenient.

7.1 Tungsten Filament Lamps

It is not difficult to provide a power supply stable enough so that the output of the bulb fluctuates by less than 1 part in 10^5. In absorption measurements, where the fractional changes in intensity are relatively small, only tungsten filament

sources have been used. On the other hand, fluorescence measurements often have larger fractional changes that will better tolerate light sources with small amounts of systematic noise, and the measured intensities are lower, making improvements in signal-to-noise ratio from brighter sources attractive.

7.2 Arc Lamps

Cairn Research Ltd (Faversham, UK) provides xenon power supplies, lamp housings, and arc lamps with noise that is in the range of 1 part in 10^4. A 150 W lamp yielded 2–3 times more light at 520 ± 45 nm than a tungsten filament bulb. The extra intensity is especially useful where the light intensity is low and the measurement is shot noise/dark noise limited (e.g. for fluorescence measurements from processes of single neurons).

7.3 Light Emitting Diodes (LEDs)

Salzberg et al. (2005) reported that high power light-emitting diodes (LED's) exhibit low-frequency noise characteristics that are clearly superior to those of tungsten halogen lamps. This holds, *a fortiori*, for arc lamps, which are generally quite poor. Also, their non-coherence is important when measuring absorption or scattering change, where the speckle from lasers is a problem (less of a problem when measuring fluorescence). In general, it is preferable to choose a single wavelength LED if this is possible, rather than filtering the output of a white LED. The former have more power in the spectral range of interest. Prizmatix, Ltd., (Givat-Shmuel, Israel) provides LED illumination systems.

7.4 Lasers

Laser illumination can provide very high illumination intensity but avoiding photodynamic damage requires careful attention to optimizing the trade-off between intensity and photodamage. The interference from speckle noise can be eliminated by reducing the beam coherence (Dejan Zecevic and Thomas Knopfel, personal communication).

8 Optics

8.1 Numerical Aperture

The need to maximize the number of measured photons has been a dominant factor in the choice of optical components. In epifluorescence, both the excitation light and the emitted light pass through the objective, and the intensity reaching the photodetector is proportional to the fourth power of numerical aperture (Inoue 1986). Clearly, numerical aperture is an important consideration in the choice of lenses. Direct comparison of the intensity reaching the image plane has shown that the light collecting efficiency of an objective is not completely determined by the stated magnification and numerical aperture. Differences of a factor of five between lenses of the same specification were found. We presume that these differences depend on the number of lenses, the coatings, and absorbances of glasses and cements. We recommend empirical tests of several lenses for efficiency.

8.2 Depth of Focus

Salzberg et al. (1977) determined the effective depth of focus for a 0.4 NA objective lens by recording an optical signal from a neuron when it was in focus and then moving the neuron out of focus by various distances. They found that the neuron had to be moved 300 μm out of focus to cause a 50 % reduction in signal size. Using 0.5 NA optics, 100 μm out of focus led to a reduction of 50 % (Kleinfeld and Delaney 1996).

8.3 Light Scattering and Out-of-Focus Light

Light scattering and out-of-focus light can limit the spatial resolution of an optical measurement. These are very large effects in measurements from mammalian brains; with wide-field microscopy individual cells cannot be imaged unless they are within 50 μm of the surface. Figure 1.8 illustrates the results of measurements carried out with a 500 μm slice of salamander cortex. The top section indicates that when no tissue is present, essentially all of the light (750 nm) from a small spot falls on one detector. The bottom section illustrates the result when the olfactory bulb slice is present. The light from the small spot is spread to about 200 μm. Mammalian cortex appears to scatter more than the salamander olfactory bulb. Clearly, light scattering causes considerable blurring of signals in vertebrate brain preparations.

The second source of blurring is signal from regions that are out of focus. For example, if the active region is a cylinder (a column) perpendicular to the plane of focus, and the objective is focused at the middle of the cylinder, then the light from

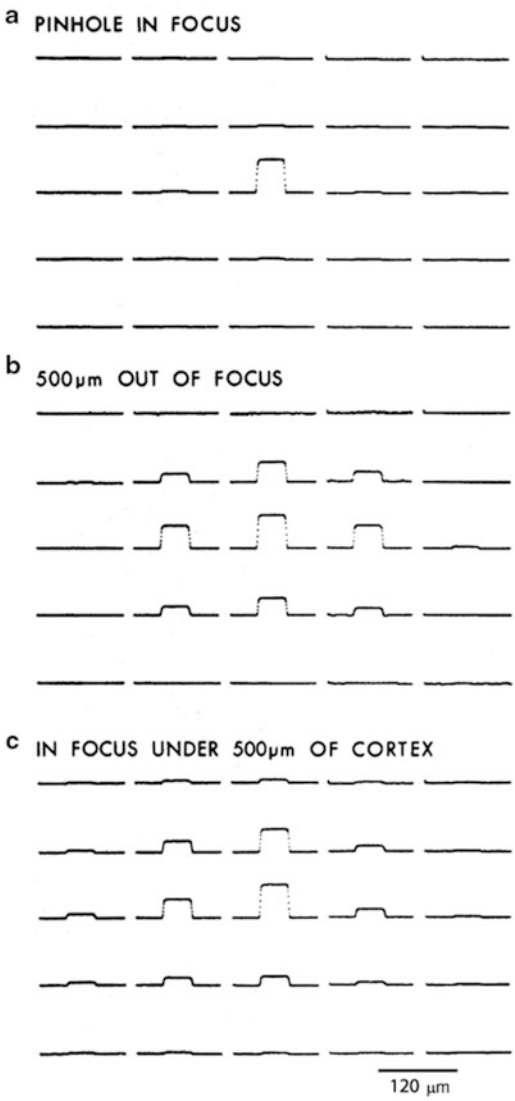

Fig. 1.8 Effects of focus and scattering on the distribution of light from a point source onto a photodetector array. (**a**) A 40 µm pinhole in aluminum foil covered with saline was illuminated with light at 750 nm. The pinhole was in focus. More than 90 % of the light fell on one detector. (**b**) The stage was moved downward by 500 µm. Light from the out-of-focus pinhole was now seen on several detectors. (**c**) The pinhole was in focus but covered by a 500 µm slice of salamander cortex. Again the light from the pinhole was spread over several detectors. A 10×0.4 NA objective was used. Kohler illumination was used. The recording gains were adjusted so the largest signal in each of the three trials would be approximately the same size in the figure. Redrawn from Orbach and Cohen (1983)

the focal plane will have the correct diameter at the image plane. However, the light from the regions above and below are out of focus and will have a diameter that is too large. The middle section of Fig. 1.8 illustrates the effect of moving the small spot of light 500 µm out of focus. The light from the small spot is spread to about 200 µm. Thus, in preparations with considerable scattering or with out-of-focus signals, the actual spatial resolution will often be limited by the preparation and not by the number of pixels in the camera.

8.4 2-Photon Microscopes

The effect of scattering and out of focus light are greatly reduced in 2-photon microscopy. However this comes with a greatly reduced fluorescence intensity. The generation of fluorescent photons in the 2-photon microscope is not efficient. We directly compared the signals from Calcium Green-1 in the mouse olfactory bulb using 2-photon and ordinary microscopy. In this comparison the number of photons contributing to the intensity measurement in the 2-photon microscope was about 1,000 times smaller than the number measured with the conventional wide-field microscope and a CCD camera. As a result the signal-to-noise ratio in the CCD recording is much larger even though the spatial resolution was much poorer (Baker et al. 2005). The factors that contribute to the relatively small number of photons in the 2-photon measurement are: (1) The incident light interacts with many fewer dye molecules because only a thin section receives high intensity illumination and (2) The presently available dyes have a low 2-photon cross section which results in a low optical efficiency. This low efficiency cannot be overcome by increasing the incident intensity because higher intensity will heat the preparation. On the other hand, the advantages of 2-photon microscopy are clear; rejection of scattered light and very shallow depth of focus results in much better x-y and z-axis resolution. The two kinds of imaging systems are optimal for different niches in the parameter space of imaging.

Table 1.1 compares the number of photons in three different kinds of measurements. A very large range of measured intensities is obtained in full frame (10,000–100,000 pixels) optical recordings from the nervous system. This range is affected both by the preparation and by the imaging method. Applications of 2-photon microscopy on voltage imaging are discussed in detail in another chapter.

8.5 Random-Access Fluorescence Microscopy

Bullen et al. (1997) have used acousto-optic deflectors to construct a random scanning microscope and were able to measure signals from parts of cultured hippocampal neurons. Relatively large signal-to-noise ratios were obtained using voltage-sensitive dyes. This method can have the advantage that only a small proportion of the preparation is illuminated, thereby reducing the photodynamic damage from the very bright laser light source. However, this method will probably be restricted to preparations such as cultured neurons where there is relatively little light scattering. Random-access fluorescence microscopy is discussed in detail in another chapter.

Table 1.1 Photons/ms/pixel

Object	Imaging method	Photons/ms/per pixel
Cell body	2-Photon fluorescence	1
Distal dendrite	Wide field fluorescence, intracellular dye, arc lamp	1,000
Brain slice	Wide field absorption	1,000,000

9 Cameras

9.1 Quantum Efficiency

Because the signal-to-noise ratio in a shot noise limited measurement is proportional to the square root of the number of photons converted into photoelectrons (see above), quantum efficiency is important. Silicon photodiodes have quantum efficiencies approaching the ideal (1.0) at wavelengths where most dyes absorb or emit light (500–800 nm). In contrast, only specially chosen vacuum photocathode devices (phototubes, photomultipliers, or image intensifiers) have a quantum efficiency as high as 0.5 and this only at certain wavelengths. Thus, in shot-noise limited situations, a silicon diode will have a larger signal-to-noise ratio. Quantum efficiencies near 1.0 in CCD and CMOS cameras are only obtained with "back illuminated" camera chips. Front illuminated chips have quantum efficiencies closer to 0.5. Photographic film has a much lower quantum efficiency, 0.01, (Shaw 1979) and thus has not been used for the kinds of measurements discussed in this book.

9.2 Imaging Devices

Perhaps the most important considerations in choosing an imaging system are the requirements for spatial and temporal resolution. Increases in either temporal or spatial resolution reduce the signal-to-noise ratio. Our discussion considers systems that have frame rates at 1 kHz or faster. In most of these systems, the camera has been placed in the objective image plane of a microscope. However, Tank and Ahmed (1985) suggested a scheme by which a hexagonal close-packed array of optical fibers is positioned in the image plane, and individual photodiodes are connected to the other end of the optical fibers. NeuroPlex-III, a 464 pixel photodiode array camera (WuTech Instruments, Gaithersburg, MD) is based on this scheme.

9.3 Silicon Diode Imagers: Parallel Readout Arrays

Diode arrays with 256–1,020 elements are used in several laboratories (e.g. Hirota et al. 1995). These arrays are designed for parallel readout; each detector followed by its own amplifier whose output can be digitized at frame rates of >1 kHz. While the need to provide a separate amplifier for each diode element limits the number of pixels in parallel read-out systems, it contributes to the very large (10^5) dynamic range that can be achieved.

9.4 CCD Cameras

By using a serial readout, the number of amplifiers is greatly reduced. In addition, it is easier to cool CCD (charge-coupled device) chips to reduce the dark noise. However, because of saturation, presently available CCD cameras are not optimal for the higher intensities available in some neurobiological experiments (Fig. 1.7). The high intensity limit of the CCD camera is set by the light intensity which fills the electron wells on the CCD chip. The well depth of commercially available CCD chips is less than 10^6 e−. This accounts for the bending over of the CCD camera performance at segment C in Fig. 1.7. A dynamic range of even 10^3 is not easily achieved with a CCD camera. A CCD camera will not be optimal for measurements of absorption (Fig. 1.7). The incident light intensity would have to be reduced with a consequent decrease in signal-to-noise ratio. On the other hand, CCD cameras are close to ideal for measurements from individual neurons stained with internally injected dyes.

9.5 CMOS Cameras

SciMedia (Taito-ku, Tokyo) and RedShirtImaging now market CMOS cameras with a well depth of 10^6 e− to 10^8 e− that are close to ideal for the range of intensities between 10^5 and 10^8 photons/msec/pixel. Table 1.2 compares a CCD camera and the CMOS cameras.

9.6 EM-CCD Cameras

These cameras have on chip multiplication and should lead to better signal to noise performance at very low light levels. However, the multiplication process adds

Table 1.2 Characteristics of three fast CCD and CMOS camera systems (as reported by the manufacturer)

	Frame rate (Hz)	Well size	Read noise	Back	Bits	
	Full frame	(×1,000 e-)	(electrons)	illum.	a-to-d	Pixels
RedShirtImaging NeuroCCD-SMQ[a]	2,000	200	20	Yes	14	80 × 80
RedShirtImaging NeuroCMOS-SM[a]	2,500, 10,000	100,000	100	No	14	128 × 128
SciMedia MiCAM Ultima[b] CMOS	10,000	1,000,000	300	No	14	100 × 100

[a] www.redshirtimaging.com
[b] www.scimedia.com

noise (a factor of 1.4) and some existing chips are even noisier than expected from the factor of 1.4. If an ordinary CCD has a read noise of 10 e−, then an ideal EM-CCD camera will have a better signal-to-noise ratio only at light levels less than 100 photons/pixel/frame. The light level achieved in the neurobiological and cardiac experiments is almost always greater than 1,000 photons/pixel/ms. Thus CCD or CMOS cameras will have a better signal-to-noise ratio than an EM-CCD.

10 Organic vs. Genetically Encoded Voltage Sensors

Organic voltage and calcium sensitive dyes stain all the cell types in the preparation. In some situations this is a positive feature but in others it is a drawback. In the vertebrate CNS the uniform staining makes it painfully difficult to determine which cell types are responsible for which components of a population signal. Similarly in a 2-photon measurement of calcium signals from cell bodies in the CNS there is no trivial way to determine which of the many cell types present are responding. In principle, a protein sensor of membrane potential or calcium would get around this problem. A variety of tools are available to obtain cell type specific expression of a protein sensor. There has been remarkable recent progress in developing protein sensors of membrane potential with larger signals a faster kinetics (see Chap. 20).

Voltage sensitive dyes were first introduced in the 1970s. Looking back, it is clear that there has been remarkable progress in the development and utilization of these tools over the past 45 years. On the other hand, from the point of view of participants in these developments, progress has seemed to be painfully slow. We should take heart from the fact that the development of the microscope continues apace after more than 400 years of effort. Voltage recording methods have already been applied to a wide variety of neurobiological and cardiac problems that range from dendritic diversity in single neurons to activity maps that cover large areas of mammalian cortex or the heart. It seems likely that new applications and tools will continue to be developed.

Acknowledgements The authors are indebted to their collaborators Bradley Baker, Vicencio Davila, Amiram Grinvald, Kohtaro Kamino, Ying-wan Lam, Leslie Loew, Bill Ross, Brian Salzberg, Alan Waggoner, Matt Wachowiak, Jian-young Wu, and Michal Zochowski for numerous discussions about optical methods.

References

Ashley CC, Ridgway EB (1970) On the relationship between membrane potential, calcium transient and tension in single barnacle muscle fibres. J Physiol 209:105–130

Baker B, Kosmidis E, Vucinic D, Falk CX, Cohen LB, Djurisic M, Zecevic D (2005) Imaging brain activity with voltage- and calcium-sensitive dyes. Cell Mol Neurobiol 25:245–282

Blasdel GG, Salama G (1986) Voltage-sensitive dyes reveal a modular organization in monkey striate cortex. Nature 321:579–585
Boyle MB, Cohen LB (1980) Birefringence signals that monitor membrane potential in cell bodies of molluscan neurons. Fed Proc 39:2130
Braddick HJJ (1960) Photoelectric photometry. Rep Prog Phys 23:154–175
Brown JE, Cohen LB, De Weer P, Pinto LH, Ross WN, Salzberg BM (1975) Rapid changes in intracellular free calcium concentration. Detection by metallochromic indicator dyes in squid giant axon. Biophys J 15:1155–1160
Bucher H, Wiegand J, Snavely BB, Beck KH, Kuhn H (1969) Electric field induced changes in the optical absorption of a merocyanine dye. Chem Phys Lett 3:508–511
Bullen A, Patel SS, Saggau P (1997) High-speed, random-access fluorescence microscopy: I. High resolution optical recording with voltage-sensitive dyes and ion indicators. Biophys J 73:477–491
Cohen LB, Keynes RD, Hille B (1968) Light scattering and birefringence changes during nerve activity. Nature 218:438–441
Cohen LB, Salzberg BM, Davila HV, Ross WN, Landowne D, Waggoner AS, Wang CH (1974) Changes in axon fluorescence during activity: molecular probes of membrane potential. J Membr Biol 19:1–36
Cohen LB, Salzberg BM (1978) Optical measurement of membrane potential. Rev Physiol Biochem Pharmacol 83:35–88
Conti F (1975) Fluorescent probes in nerve membranes. Annu Rev Biophys Bioeng 4:287–310
Conti F, Tasaki I, Wanke E (1971) Fluorescence signals in ANS-stained squid axons during voltage clamp. Biophys J 8:58–70
Davila HV, Cohen LB, Salzberg BM, Shrivastav BB (1974) Changes in ANS and TNS fluorescence in giant axons from *Loligo*. J Membr Biol 15:29–46
Fromherz P, Dambacher KH, Ephardt H, Lambacher A, Muller CO, Neigl R, Schaden H, Schenk O, Vetter T (1991) Fluorescent dyes as probes of voltage transients in neuron membranes: progress report. Ber Bunsenges Phys Chem 95:1333–1345
Garaschuk O, Milos RI, Grienberger C, Marandi N, Adelsberger H, Konnerth A (2006) Optical monitoring of brain function in vivo: from neurons to networks. Pflugers Arch 453:385–396
Grinvald A, Lieke E, Frostig RD, Gilbert CD, Wiesel TN (1986) Functional architecture of cortex revealed by optical imaging of intrinsic signals. Nature 324:361–364
Gross E, Bedlack RS, Loew LM (1994) Dual-wavelength ratiometric fluorescence measurements of the membrane dipole potential. Biophys J 67:208–216
Gupta RK, Salzberg BM, Grinvald A, Cohen LB, Kamino K, Lesher S, Boyle MB, Waggoner AS, Wang CH (1981) Improvements in optical methods for measuring rapid changes in membrane potential. J Membr Biol 58:123–137
Hill DK (1950) The effect of stimulation on the opacitiy of a crustacean nerve trunk and its relation to fibre diameter. J Physiol 111:283–303
Hill DK, Keynes RD (1949) Opacity changes in stimulated nerve. J Physiol 108:278–281
Hirota A, Sato K, Momose-Sato Y, Sakai T, Kamino K (1995) A new simultaneous 1020-site optical recording system for monitoring neural activity using voltage-sensitive dyes. J Neurosci Methods 56:187–194
Inoue S (1986) Video microscopy. Plenum, New York
Jobsis FF, O'Connor MJ (1966) Calcium release and reabsorption in the sartorius muscle of the toad. Biochem Biophys Res Commun 25:246–252
Kleinfeld D, Delaney KR (1996) Distributed representation of vibrissa movement in the upper layers of somatosensory cortex revealed with voltage-sensitive dyes. J Comp Neurol 375:89–108
Labhart H (1963) Bestimmung von moleküleigenschaften aus elektrooptischen effekten. Tetrahedron 19(Suppl 2):223–241
Levin SV, Rosenthal DL, Komissarchik YY (1968) Structural changes in the axon membrane on excitation. Biofizika 13:180–182

Loew LM, Cohen LB, Salzberg BM, Obaid AL, Bezanilla F (1985) Charge-shift probes of membrane potential. Characterization of aminostyrylpyridinium dyes on the squid giant axon. Biophys J 47:71–77

London JA, Zecevic D, Cohen LB (1987) Simultaneous optical recording of activity from many neurons during feeding in *Navanax*. J Neurosci 7:649–661

Malmstadt HV, Enke CG, Crouch SR, Harlick G (1974) Electronic measurements for scientists. Benjamin, Menlo Park, CA

Maylie J, Irving M, Sizto NL, Boyarsky G, Chandler WK (1987) Calcium signals recorded from cut frog twitch fibers containing tetramethylmurexide. J Gen Physiol 89:145–176

Nasonov DN, Suzdal'skaia IP (1957) Changes in the cytoplasm of myelinated nerve fibers during excitation. Fiziol Zh SSSR 43:664–672

Orbach HS, Cohen LB (1983) Optical monitoring of activity from many areas of the *in vitro* and *in vivo* salamander olfactory bulb: a new method for studying functional organization in the vertebrate central nervous system. J Neurosci 3:2251–2262

Orbach HS, Cohen LB, Grinvald A (1985) Optical mapping of electrical activity in rat somatosensory and visual cortex. J Neurosci 5:1886–1895

Ross WN, Salzberg BM, Cohen LB, Davila HV (1974) A large change in dye absorption during the action potential. Biophys J 14:983–986

Ross WN, Salzberg BM, Cohen LB, Grinvald A, Davila HV, Waggoner AS, Wang CH (1977) Changes in absorption, fluorescence, dichroism, and birefringence in stained giant axons : optical measurement of membrane potential. J Membr Biol 3:141–183

Salzberg BM, Bezanilla F (1983) An optical determination of the series resistance in Loligo. J Gen Physiol 82:807–817

Salzberg BM, Grinvald A, Cohen LB, Davila HV, Ross WN (1977) Optical recording of neuronal activity in an invertebrate central nervous system: simultaneous monitoring of several neurons. J Neurophysiol 40:1281–1291

Salzberg BM, Kosterin PV, Muschol M, Obaid AL, Rumyantsev SL, Bilenko Y, Shur MS (2005) An Ultra-stable non-coherent light source for optical measurements in neuroscience and cell physiology. J Neurosci Methods 141:165–169

Schuette WH, Whitehouse WC, Lewis DV, O'Connor M, VanBuren JM (1974) A television fluorimeter for monitoring oxidative metabolism in intact tissue. Med Instrum 8:331–333

Shaw R (1979) Photographic detectors. Appl Opt Optical Eng 7:121–154

Svoboda K, Denk W, Kleinfeld D, Tank DW (1997) In vivo dendritic calcium dynamics in neocortical pyramidal neurons. Nature 385:161–165

Tank D, Ahmed Z (1985) Multiple-site monitoring of activity in cultured neurons. Biophys J 47:476A

Tasaki I, Watanabe A, Sandlin R, Carnay L (1968) Changes in fluorescence, turbidity, and birefringence associated with nerve excitation. Proc Natl Acad Sci U S A 61:883–888

Tsien RY (1989) Fluorescent probes of cell signaling. Annu Rev Neurosci 12:227–253

Vereninov AA, Nikolsky NN, Rosenthal DL (1962) Neutral red sorption by the giant axon of Sepia at excitation. Tsitologiya 4:666–668

Wachowiak M, Cohen LB (2003) Correspondence between odorant-evoked patterns of receptor neuron input and intrinsic optical signals in the mouse olfactory bulb. J Neurophysiol 89:1623–1639

Waggoner AS, Grinvald A (1977) Mechanisms of rapid optical changes of potential sensitive dyes. Ann N Y Acad Sci 303:217–241

Wu JY, Cohen LB (1993) Fast multisite optical measurements of membrane potential. In: Mason WT (ed) Fluorescent and luminescent probes for biological activity. Academic Press, London, pp 389–404